Biometals (2012) 25:435–450
DOI 10.1007/s10534-011-9516-4

Association of aureolic acid antibiotic, chromomycin A3 with Cu^{2+} and its negative effect upon DNA binding property of the antibiotic

Shibojyoti Lahiri · Toshifumi Takao · Pukhrambam Grihanjali Devi · Saptaparni Ghosh · Ayanjeet Ghosh · Amrita Dasgupta · Dipak Dasgupta

Received: 28 October 2011 / Accepted: 14 December 2011 / Published online: 29 December 2011

Abstract Here we have examined the association of an aureolic acid antibiotic, chromomycin A3 (CHR), with Cu^{2+}. CHR forms a high affinity 2:1 (CHR:Cu^{2+}) complex with dissociation constant of 0.08×10^{-10} M^2 at 25°C, pH 8.0. The affinity of CHR for Cu^{2+} is higher than those for Mg^{2+} and Zn^{2+} reported earlier from our laboratory. CHR binds preferentially to Cu^{2+} in presence of equimolar amount of Zn^{2+}. Complex formation between CHR and Cu^{2+} is an entropy driven endothermic process. Difference between calorimetric and van't Hoff enthalpies indicate the presence of multiple equilibria, supported from biphasic nature of the kinetics of association. Circular dichroism spectroscopy show that [$(CHR)_2$:Cu^{2+}] complex assumes a structure different from either of the Mg^{2+} and Zn^{2+} complex reported earlier. Both [$(CHR)_2$:Mg^{2+}] and [$(CHR)_2$:Zn^{2+}] complexes are known to bind DNA. In contrast, [$(CHR)_2$:Cu^{2+}] complex does not interact with double helical DNA, verified by means of Isothermal Titration Calorimetry of its association with calf thymus DNA and the double stranded decamer (5′-CCGGCGCCGG-3′). In order to interact with double helical DNA, the $(antibiotic)_2$: metal (Mg^{2+} and Zn^{2+}) complexes require a isohelical conformation. Nuclear Magnetic Resonance spectroscopy shows that the Cu^{2+} complex adopts a distorted octahedral structure, which cannot assume the required conformation to bind to the DNA. This report demonstrates the negative effect of a bivalent metal upon the DNA binding property of

Electronic supplementary material The online version of this article (doi:10.1007/s10534-011-9516-4) contains supplementary material, which is available to authorized users.

S. Lahiri · P. G. Devi · S. Ghosh · A. Ghosh · A. Dasgupta · D. Dasgupta (✉)
Biophysics Division, Saha Institute of Nuclear Physics, 1/AF Bidhannagar, Sector – 1, Kolkata 700064, India
e-mail: dipak.dasgupta@saha.ac.in

T. Takao
Laboratory of Protein Profiling and Functional Proteomics, Institute for Protein Research (IPR), Osaka University, 3-2 Yamadaoka, Suita-shi, Osaka 565-0871, Japan

Present Address:
P. G. Devi
Department of Chemistry, Imphal College, Imphal, Manipur, India

Present Address:
A. Ghosh
Department of Chemistry, University of Pennsylvania, 231 South 34th Street, Philadelphia, PA 19104, USA

Present Address:
A. Dasgupta
National Centre for Biological Sciences (NCBS), Tata Institute of Fundamental Research (TIFR), Bangalore 560065, India

CHR, which otherwise binds to DNA in presence of metals like $Mg^{2+}$and Zn^{2+}. The results also indicate that CHR has a potential for chelation therapy in Cu^{2+} accumulation diseases. However cytotoxicity of the antibiotic might restrict the use.

Keywords Chromomycin · Copper ion · Electrospray ionization mass spectrometry · Multiple equilibria · DNA binding · Distorted octahedral structure

Introduction

Chromomycin (CHR) (Fig. 1) is a naturally occurring aureolic acid group of antibiotic synthesized by the bacteria *Streptomyces griseus* (Lombo et al. 2006). It binds via minor groove of DNA with GC-base specificity in presence of bivalent metal ions like Mg^{2+} and thereby inhibits replication and transcription (Aich et al. 1992b; Behr et al. 1969; Cons and Fox 1989). Inhibition of DNA dependent RNA synthesis by the antibiotic, both in vivo and in vitro, has been proposed to be the major cause for its antibiotic and anticancer activity (Baguley 1982). The requirement of bivalent metal ions for the biological activity of CHR originates from its affinity for bivalent metal ions. Association of this antibiotic with bivalent metal ions and the properties of those antibiotic:metal complexes has been demonstrated for metal ions like Mg^{2+}, Co^{2+}, Zn^{2+}, Ni^{2+}, etc. (Aich et al. 1992a; Devi et al. 2007; Gochin 1998; Reyzer et al. 2001). Previous studies from our laboratory have shown that CHR forms complexes with Mg^{2+} and Zn^{2+} (Aich et al. 1992a; Devi et al. 2007). The antibiotic forms two different types of complexes (1:1 and 1:2) with Mg^{2+} depending on Mg^{2+} concentration (Aich et al. 1992a). These are the DNA binding ligands (Chakrabarti et al. 2000). In contrast, it forms only a single type of complex with Zn^{2+} (Devi et al. 2007). Renewed studies to explore alternative therapeutic potential of generic drugs like CHR/MTR have led us to suggest alternate probable targets of the antibiotics within the cell (Chakraborty et al. 2008; Sleiman et al. 2011).

Considering the metal binding property of CHR, we have studied its binding ability with an essential, but potentially harmful micronutrient Cu^{2+}. Copper is an important trace element of the human body. It takes part in the sustenance of various organs and tissues of human body. Its functions in the body include processes such as making neurotransmitters, formation of collagen in bones and muscles and maintenance of the immune system and elasticity of blood vessels and cardiac muscles (Olivares and Uauy 1996). Homeostasis of copper is very important, because conditions of copper deficiency as well as that of its excess lead to adverse health conditions. Copper accumulation has been implied in the etiopathogeneses of Wilson's disease and neurodegenerative disorders such as Alzheimer's disease, Prion disease including Bovine Spongiform Encephalopathy (BSE) (Waggoner et al. 1999). Excess of copper has also been found to increase oxidative stress and aging. Recently, copper accumulation has been linked to cancer and tumor progression as well (Valko et al. 2006). Therefore, compounds with the potential to bind Cu^{2+} with a relatively high affinity might be putative therapeutic agents for these diseases (Daniel et al. 2004). There are reports to show that use of compounds like Clioquinol (Cu^{2+}/Zn^{2+} chelator) reduces the physiological effect of Alzheimer's disease (Di Vaira et al. 2004).

We have studied in depth the complex formation between CHR with Cu^{2+}. We have characterized the binding, and reported the structure of the Cu^{2+} complex. These studies have led to understand its mechanism of binding with Cu^{2+}. The mode of association of CHR with three important metal ions, Mg^{2+}, Zn^{2+} and Cu^{2+} have been compared. Keeping in view the earlier reports of [$(CHR)_2$: metal ion] complexes as active DNA binding agents, we have demonstrated the inability of [CHR:Cu^{2+}] complex to bind double helical DNA. This is a unique feature which has not been hitherto reported for any other

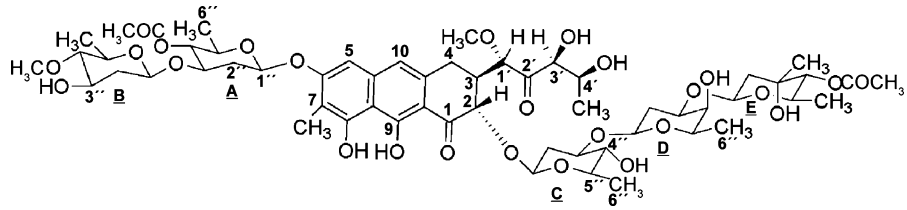

Fig. 1 Chemical structure of chromomycin A3

metal ion dependent antibiotic. In the end, the physiological implications of the results have been addressed.

Materials and methods

Materials

$CuSO_4.5H_2O$ and Hydrochloric acid (HCl) [ACS grade] were purchased from Merck, Germany. Chromomycin (CHR) was purchased from Sigma Chemical Co. and M.P. Biomedicals, USA. Calf thymus DNA, HPLC purified DNA oligomer (5′-CCGGCGCCGG-3′), Trizma base, K_2HPO_4 and KH_2PO_4 were purchased from Sigma Chemical Co., USA.

Methods

Absorbance spectroscopy

Absorbance spectra were recorded in a Cecil CE7500 spectrophotometer. Concentration of CHR was calculated considering the molar extinction coefficient of $8.8 \times 10^3\ M^{-1}\ cm^{-1}$ for CHR at 405 nm.

Fluorescence spectroscopy

Fluorescence spectra were recorded in a Perkin-Elmer LS55 luminescence spectrometer. 10 μM CHR was excited at 470 nm and the corresponding fluorescence emission was recorded over the range of 500–650 nm. Both the excitation and emission slit widths were kept fixed at 10 nm each. The recorded spectra were an average of four scans. Titrations were performed under similar conditions at different temperatures (25, 30, 35 and 40°C) to obtain thermodynamic parameters by van't Hoff's method.

Stopped flow kinetics

The kinetics of the association of CHR with Cu^{2+} was followed using a SFA-20 Rapid Kinetics accessory (Hi-Tech Scientific) attached to a Perkin-Elmer LS55 luminescence spectrometer. The reactants were mixed in equal volumes and the change in fluorescence intensity at 540 nm ($\lambda_{ex} = 470$ nm) associated with the formation of the complex was followed as function of time after an initial lapse of 20 ms. Data from four independent runs were accumulated in the final data analysis. The obtained kinetic traces, could best be fitted with the following equation.

$$y = A_1 e^{-k_1 t} + A_2 e^{-k_2 t} \quad (1)$$

where, y is the spectroscopic property being monitored (fluorescence intensity at 540 nm in this case), A_1 and A_2 are the amplitude factors for the first and the second steps respectively and k_1 and k_2 are the rate constants for the same two steps.

Circular dichroism (CD) spectroscopy

The CD spectra were recorded in a Jasco J720 spectropolarimeter using a quartz cuvette of 1 cm path length. CD spectra in the near UV and visible region were recorded on addition of increasing concentrations of Cu^{2+} to a fixed concentration of CHR (10 μM). Reported spectra were an average of four scans. The observed data points were subsequently smoothed and analysed using the Jasco CD Standard Analysis software.

Electrospray ionization mass spectrometry (ESI–MS)

All mass spectrometric measurements were carried out on a Q-TOF mass spectrometer (Micromass, Manchester, U.K.), which is a hybrid quadrupole orthogonal acceleration tandem mass spectrometer, fitted with a Z-spray nanoflow electrospray ion source. Stable isotopes, ^{68}ZnO (99 at.%) and $^{63}CuCl_2$ (99 at.%), were obtained from Taiyo Nippon Sanso (Tokyo, Japan), and used for the association with CHR. This eliminated peak broadening derived from the natural isotopes of Zn and Cu. CHR solution was prepared in 10 mM NH_4HCO_3 buffer, pH 8.0. A solution containing 50 μM CHR and 100 μM $^{63}CuCl_2$ was mixed well, filtered and mounted on the platform in a nanoflow needle for subsequent measurements. Similar protocol was followed to assess the competitive binding potential of Cu^{2+} and Zn^{2+} ions with CHR. In this case, the experimental solution contained 50 μM CHR and a mixture of 100 μM $^{63}CuCl_2$ and 100 μM ^{68}ZnO. The observed mass was then compared with the theoretically calculated monoisotopic mass and isotopic distribution of the [CHR-Cu^{2+}] complex. Theoretical calculation of the metal complexes was carried out by Isotopica (http://coco.protein.osaka-u.ac.jp/Isotopica/), a software aid for

calculating and analyzing complex isotopic envelopes (Fernandez-de-Cossio et al. 2004).

^{1}H NMR spectroscopy

1D and 2D (NOESY and COSY) NMR spectra for CHR (1 mM) and CHR-Cu^{2+} (700 μM Cu^{2+}) complexes were recorded at 25°C, pH 8.0 in a Bruker 600 Ultra Shield NMR machine. 10% D_2O was used for external locking. The 2D spectra were recorded for 16 h. A mixing time of 400 ms was used in each case. All samples were prepared in 20 mM potassium phosphate buffer (pH 8.0). Data were analyzed with Bruker TopSpin 1.3 software.

Preparation of the DNA oligomer

HPLC purified and desalted self-complimentary oligonucleotide (5′-CCGGCGCCGG-3′) was purchased from Sigma Chemical Company, USA and was used without further purification. Lyophilized DNA was dissolved in 20 mM Tris–HCl buffer, pH 8.0, vortexed and left at room temperature for 30 min. It was then heated to 70°C, kept for 10 min and allowed to equilibrate slowly to room temperature. The sample was subsequently stored at 4°C. Duplex concentration was estimated spectrophotometrically using a molar absorption coefficient (ε) of 161.85×10^3 M^{-1} cm^{-1} at 260 nm (calculated by nearest neighbor approximation method).

Isothermal titration calorimetry (ITC)

(i) Calorimetric titrations were performed in a VP-ITC microcalorimeter with CHR (20 μM) in the cell. Increasing concentrations of Cu^{2+} (stock concentration of 700 μM) were added from the syringe. The titrations and control experiments were performed at 25°C. For control experiments, same amount of Cu^{2+} was added to the buffer (10 mM Tris–HCl, pH 8.0) in the cell.

(ii) To monitor the interaction of the copper complex with calf thymus DNA (ct DNA), [$(CHR)_2$:Cu^{2+}] complex (30 μM CHR preincubated with 150 μM Cu^{2+}) were titrated against deproteinised ct DNA (stock concentration of 1.7 mM) containing same amount of Cu^{2+}. The titrations and control experiments were performed at 25°C. For control experiments, same amount of ct DNA (containing 150 μM Cu^{2+}) was added to buffer containing same amount of Cu^{2+}. Titrations under similar conditions were done to evaluate the thermodynamic parameters for the association of [$(CHR)_2$:Zn^{2+}] complex (30 μM CHR preincubated with 600 μM Zn^{2+}) and ct DNA containing same amount of Zn^{2+}. Above samples were dissolved in 10 mM Tris–HCl buffer, pH 8.0 and all experiments were performed at 25°C.

(iii) To examine the interaction of [$(CHR)_2$:Cu^{2+}] (30 μM CHR preincubated with 150 μM Cu^{2+}) and [$(CHR)_2$:Zn^{2+}] (30 μM CHR preincubated with 600 μM Zn^{2+}) complexes with the double stranded oligomer 5′-CCGGCGCCGG-3′, the metal complexes (taken in the cell of ITC_{200} microcalorimeter) were titrated against increasing concentration of the oligomer (stock concentration of 600 μM taken in the syringe) containing same amounts of Cu^{2+} and Zn^{2+}. As control, same amount of oligomer (containing 150 μM Cu^{2+} and 600 μM Zn^{2+}) was added to buffer containing 150 μM Cu^{2+} and 600 μM Zn^{2+} respectively. All experiments were carried out in 20 mM Tris–HCl buffer, pH 8.0 at 25°C.

Analysis

Evaluation of binding stoichiometry of CHR with Cu^{2+}

The method of continuous variation was employed to determine binding stoichiometry of the complex of CHR with Cu^{2+}. Absorbance of CHR at 405 nm was recorded at a constant temperature (25°C) for reaction mixtures, in which number of moles of CHR and Cu^{2+} in a fixed volume were varied, keeping the sum total number of moles and the reaction volume constant. Absorbance of CHR under these conditions was plotted as a function of the input mole fraction of CHR. The point in the plot where the two straight lines meet, corresponds to the mole fraction of the antibiotics in the antibiotic:Cu^{2+} complex. The stoichiometry is obtained in terms of the antibiotic:Cu^{2+} [χ_{ligand}:(1- χ_{ligand})], where χ_{ligand} is the mole fraction of the antibiotic calculated as the ratio of the molar concentration of antibiotics to the total molar concentration of antibiotic and Cu^{2+}.

Further support for the existence of a complex between the antibiotic and $Cu^{2+}$and evaluation of the binding stoichiometry were obtained by means of ESI–MS measurements.

Fluorescence spectroscopy to evaluate the dissociation constant K_d for the complex between CHR and Cu^{2+}

A fixed concentration of CHR (10 μM) was taken in a cuvette (1 cm path length) and titrated with increasing concentrations of Cu^{2+}. All samples were dissolved in 10 mM Tris–HCl buffer, pH 8.0 and the experiments were performed at room temperature (25°C). The affinity between CHR and Cu^{2+} was determined by two methods discussed below.

Method 1

Apparent dissociation constant (K_{app}) was estimated from the concentration of Cu^{2+} required for 50% binding of the antibiotics, i.e. the half saturation value obtained from a plot of fraction of CHR bound against the input concentration of Cu^{2+}.

Method 2

This method takes into account the reaction stoichiometry (2:1 in terms of CHR and Cu^{2+}) in order to evaluate the true dissociation constant K_d. The method of analysis is described below:

$$2D + Cu^{2+} \leftrightarrow (D_2)Cu^{2+} \tag{2}$$

At equilibrium, the dissociation constant K_d (according to the law of mass action) is given by

$$K_d = \frac{[D]^2[Cu^{2+}]}{[(D)_2Cu^{2+}]} \tag{3}$$

where, species in square brackets indicate the respective molar concentrations at equilibrium. Therefore the concentrations of the unbound drug and metal ions at equilibrium can be described as

$$[D]_f = [D]_0 - 2[(D)_2Cu^{2+}] \tag{4}$$

$$[Cu^{2+}]_f = [Cu^{2+}]_i - 2[(D)_2Cu^{2+}] \tag{5}$$

where $[D]_0$ is the initial drug concentration and $[Cu^{2+}]_i$ is the added Cu^{2+} concentration in solution. So, the fraction of antibiotics bound is given by

$$\alpha = \frac{2[(D)_2Cu^{2+}]}{[D]_0} \tag{6}$$

Substituting the value of $2[(D)_2Cu^{2+}]$ obtained from Eq. 5 in Eqs. 3 and 4, we get

$$[D]_f = [D]_0(1 - \alpha) \tag{7}$$

and,

$$[Cu^{2+}]_f = [Cu^{2+}]_i - \frac{\alpha[D]_0}{2} \tag{8}$$

Substituting Eqs. 6 and 7 in Eq. 2, we get

$$K_d = \frac{[D]_0(1-\alpha)^2(2[Cu^{2+}]_i - \alpha[D]_0)}{\alpha}. \tag{9}$$

van't Hoff's method

Thermodynamic parameters ΔH (van't Hoff's enthalpy), ΔS (change in entropy) and ΔG (change in Gibb's free energy) for the complexation reaction, were also calculated using the following equations:

$$\Delta G = -RT \ln \frac{1}{K_{app}} \tag{10}$$

$$\frac{d(\ln \frac{1}{K_{app}})}{dT} = -\frac{\Delta H}{RT^2} \tag{11}$$

$$\Delta G = \Delta H - T\Delta S \tag{12}$$

where, R and T are the universal gas constant and absolute temperature respectively. The thermodynamic parameters are obtained from the plot of $ln(1/K_{app})$ versus $1/T$, the slope of which gives the van't Hoff's enthalpy and change in entropy is obtained from the intercept.

Results

Formation of (CHR):Cu^{2+} complex

Association of CHR with Cu^{2+} was demonstrated by absorbance spectroscopy. Upon addition of Cu^{2+} there is a decrease in absorbance of CHR at 405 nm (Fig. 2a). Concomitant broadening of the spectra and a red shift of the peak with increasing input concentrations of Cu^{2+} (Fig. 2a) characterize the change. There is also a decrease in the absorbance at 280 nm and shift towards the longer wavelength in the UV region. The changes in the absorption spectrum of

CHR upon addition of Cu^{2+} are a result of the complex formation between them. The appearance of a new absorbance band around 440 nm is a signature of metal complexation by CHR (Aich et al. 1992a; Devi et al. 2007). Presence of an isosbestic point at 423 nm for CHR indicates the presence of a single type of [CHR:Cu^{2+}] complex over the input concentration range of copper. The fluorescence emission spectrum of CHR is also quenched along with a broadening of the emission spectra on addition of increasing concentrations of Cu^{2+} (Fig. 2b).

Stoichiometry of the (CHR): Cu^{2+} complex

The plot obtained from the continuous variation method for the formation of CHR:Cu^{2+} complex is shown in Fig. 3. The point of inflection is at $\chi_{ligand} = 0.67$. It suggests a stoichiometry of 2:1 with respect to CHR:Cu^{2+}. Therefore, the composition of the complex is [$(CHR)_2$:Cu^{2+}].Further characterization and evaluation of the composition of the complex were done using ESI–MS. CHR was observed as a monomer associated with an ammonium ion to form a singly charged ion (Fig. 4a). Meanwhile, in the presence of Cu^{2+}, it formed a stable dimer, [$(CHR)_2$:Cu^{2+}] and tetramer [$(CHR)_2$:$Cu^{2+}]_2$ coordinated with one and two Cu^{2+} ions, respectively, which were observed as doubly- and triply-charged ions. In addition, the MS/MS of the tetramer ion at *m/z* 1635.4 clearly gave a dimer at *m/z* 1231.0 and further degraded product ion (CHR $-H^+ + Cu^{2+}$) at *m/z* 1244.5, which supported the existence of the tetramer in the present preparation (Fig. 4c; Table 1). These observations demonstrate the formation of a [$(CHR)_2$:Cu^{2+}] complex.

Binding parameters for the association of CHR with Cu^{2+}

The affinity constant for complex of CHR with Cu^{2+} was evaluated using the method described under the Analysis Section. ΔF represents the change in fluorescence intensity at 540 nm ($\lambda_{ex.} = 470$ nm), whereas ΔF_{max} denotes the change in fluorescence intensity when Cu^{2+} is completely bound to the antibiotics. Therefore, $\Delta F/\Delta F_{max}$ denotes the fraction of CHR bound to Cu^{2+}. K_d is estimated from each data point (using Eq. 8) in this fraction bound versus Cu^{2+} concentration plots (Fig. 5). Using Eq. 8, K_d at each observed data point (α, $[Cu^{2+}]_i$) was calculated and the reported K_d value is the average over entire input concentration range of Cu^{2+}. Comparison of the dissociation constant value for [$(CHR)_2$:Cu^{2+}] complex (Table 2) with those of other metal complexes like Mg^{2+} and Zn^{2+} (Chakraborty et al. 2008) show that CHR binds to Cu^{2+} with a relatively high affinity.

Preferential association of CHR with Cu^{2+}

Figure 6a–c shows the mass spectra of solutions containing CHR, CHR and $^{63}CuCl_2$, and CHR and equimolar amounts of $^{63}CuCl_2$ and ^{68}ZnO, respectively. The results clearly indicate that CHR forms the same complex with an equimolar mixture of $^{63}CuCl_2$ and ^{68}ZnO (Fig. 6c) as with $^{63}CuCl_2$ alone (Fig. 6b). It supports preferential binding to Cu^{2+}.

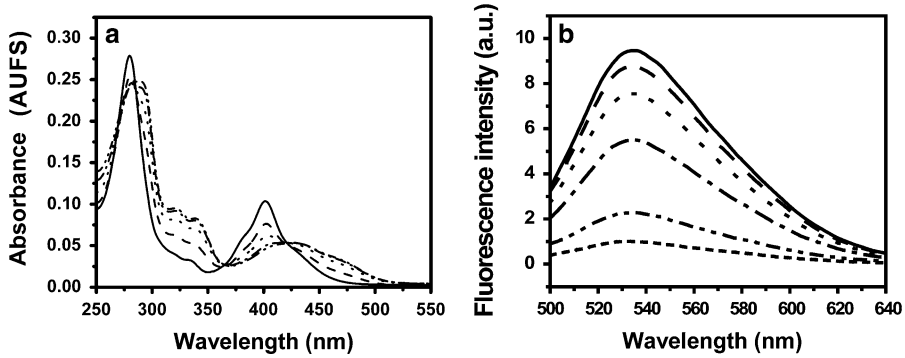

Fig. 2 **a** Absorbance spectra of 10 μM CHR (*solid line*) and on addition of 6 μM (*dashed line*), 10 μM (*dotted line*), 30 μM (*dashed dotted line*), and 100 μM (*dashed double dotted line*) Cu^{2+} **b** Fluorescence spectra of 10 μM CHR (*solid line*) and on addition of 5 μM (*dashed line*), 10 μM (*dotted line*), 20 μM (*dashed dotted line*), 50 μM (*dashed double dotted line*) and 100 μM (*short dashed line*) Cu^{2+}. All spectra were recorded at room temperature (25°C) in 10 mM Tris–HCl buffer, pH 8.0

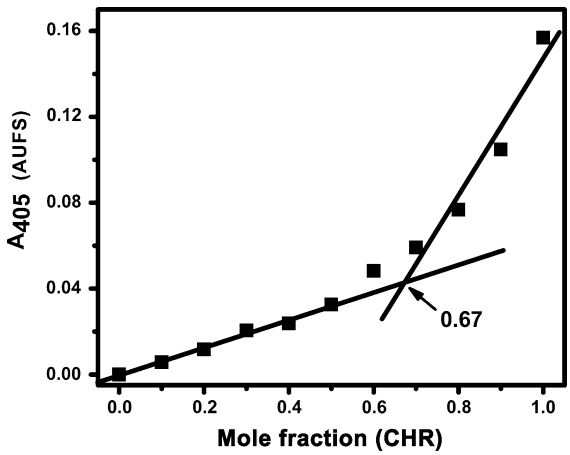

Fig. 3 Plot of continuous variation for association of CHR with Cu^{2+}. Absorption was measured at 25°C in 10 mM Tris–HCl, pH 8.0

Thermodynamics of complex formation of CHR with Cu^{2+}

The enthalpy change for the complex formation of CHR with Cu^{2+} after subtracting the heat change due to dilution of Cu^{2+} is shown in Fig. 7a. The experimental data points could be best fitted with 'one set of sites' model provided with the Microcal LLC software (supplied by the manufacturer). Values for thermodynamic parameters (Table 3) show that the complex formation is predominantly entropy driven. The reaction is endothermic in nature, with a positive change in enthalpy. Apparent dissociation constant (Table 3) shows a micromolar order of affinity. K_{app} obtained from fluorimetric titration is also comparable with that obtained from calorimetric measurements at 25°C (Table 3).

van't Hoff's plot (Fig. 7b) of the variation of affinity constant with temperature shows that the complexation reaction is exothermic at higher temperatures. The values of calorimetric and van't Hoff's enthalpy and entropy are significantly different (Table 3).

Kinetics of the association of CHR with Cu^{2+}

Figure 8 shows the representative kinetic trace for the association of CHR with Cu^{2+}. The data shown here is an average of four independent runs (Online Resource, Table OR1), each of which could be best fitted to a biphasic rate equation with average rate constant values of $(17.5 \pm 0.57) \times 10^{-3}$ and $(7.25 \pm 1.17) \times 10^{-4}$ s^{-1} for the faster and the slower steps, respectively. The amplitude factors ($A_1 = 2.3 \pm 0.25$ and $A_2 = 0.15 \pm 0.008$), for the faster and the slower steps are 93.9% and 6.1%, respectively. The slower step with small intensity has been suggested from a statistical analysis of data from four runs.

Interaction of $[(CHR)_2:Cu^{2+}]$ and $[(CHR)_2:Zn^{2+}]$ complexes with DNA

As is evident from the thermogram (Fig. 9a), the heat change for the interaction of the copper complex with increasing concentrations of ct DNA has near constant

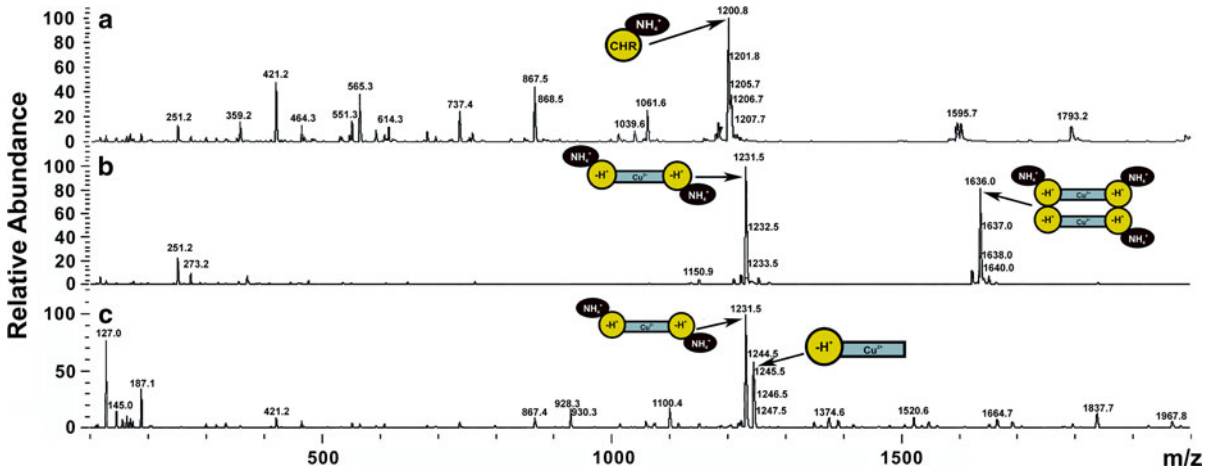

Fig. 4 **a** ESI–MS profile of unbound CHR (50 μM) in 10 mM NH_4HCO_3 buffer, pH 8.0 **b** ESI–MS profile of $[(CHR)_2:Cu^{2+}]$ in 10 mM NH_4HCO_3 buffer, pH 8.0. **c** MS/MS profile of the oddly charged peak ($m/z = 1636.0$) present in panel B. The *circles* represent the CHR molecule, *rectangles* represent Cu^{2+} and *ovals* are representative of NH_4^+ ions

Table 1 Mass spectrometric determination of the molecular species formed by CHR and Cu^{2+} in solution

Molecule	Formula	Observed *m/z*	Calculated mass (Da)
CHR	$C_{57}H_{82}O_{26}$	–	1182.5
$(CHR)NH_4^{+a}$		1200.7 (+1)	1200.5
$(2CHR + Cu\text{-}2H^+)2NH_4^{+b}$		1231.0 (+2)	2462.0
$(2CHR + Cu\text{-}2H^+)_23NH_4^{+c}$		1635.4 (+3)	4906.0
$(CHR + Cu\text{-}H^+)^d$		1244.5 (+1)	1244.4

ESI–MS analysis for CHR and the [CHR:Cu^{2+}] complex and comparison with theoretically estimated masses

[a] Refer to Figs. 4a and 6a

[b] Refer to Figs. 4b, c, and 6b, c

[c] Refer to Figs. 4b, and 6b, c

[d] Refer to Fig. 4c

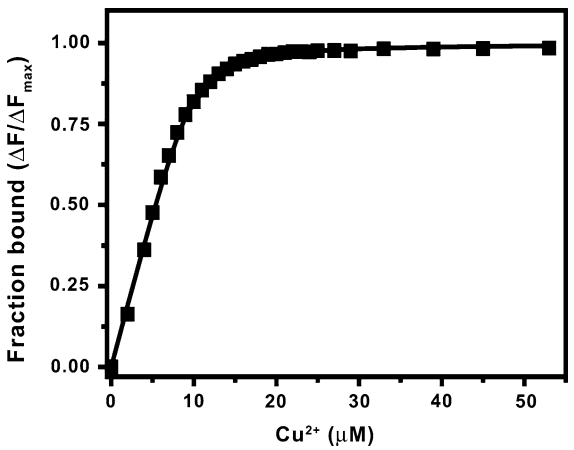

Fig. 5 Binding isotherm for the association of CHR with Cu^{2+} as determined from fluorescence titration. CHR was excited at 470 nm and the corresponding emission at 540 nm was recorded at 25°C in 10 mM Tris–HCl, pH 8.0

Table 2 Affinity of CHR for Cu^{2+}, Zn^{2+} and Mg^{2+}

System	Dissociation constants (K_d), M^2 ($\times 10^{-10}$)
CHR:Cu^{2+}	0.08
CHR:Zn^{2+}	3.2
CHR:Mg^{2+}	9,100

Dissociation constants for [$(CHR)_2$:Cu^{2+}], [$(CHR)_2$:Zn^{2+}] and [$(CHR)_2$:Mg^{2+}] complexes as determined by optical spectroscopy at 25°C

The K_d values for the formation of [$(CHR)_2$:Zn^{2+}] and [$(CHR)_2$:Mg^{2+}] complexes are cited from (Chakraborty et al. 2008)

values, which are scattered around the zero line in the normalized ΔH plots. This indicates that Cu^{2+} complex of the antibiotics do not interact with double stranded DNA. The thermogram and the calculated thermodynamic parameters under similar conditions for the Zn^{2+} complex are shown for comparison in Fig. 9b; Table 4. The K_{app} value obtained from this calorimetric titration is of the same order (Table 4) as reported earlier from our laboratory for the structurally related antibiotic Mithramycin (MTR) (Das and Dasgupta 2005). In contrast, [$(CHR)_2$:Cu^{2+}] complex does not interact with double stranded DNA, even when presented with defined binding motifs like CCG, GCC, etc.(Van Dyke and Dervan 1983) (present in the DNA decamer 5′-CCGGCGCCGG-3′) (Online Resource, Fig. OR1A). The best fit curve obtained provides absurd parameters for the interaction of [$(CHR)_2$:Cu^{2+}] complex with the DNA decamer, as is evident from Fig. OR1A. On the other hand [$(CHR)_2$:Zn^{2+}] complex interacts with the same sequence under similar conditions (Online Resource, Fig. OR1B) with thermodynamically favorable parameters (Online Resource, Table OR2). Absence of the association between DNA and [$(CHR)_2$:Cu^{2+}] complex indicate that the metal complex might adopt a geometry different from that of [$(CHR)_2$:Zn^{2+}] complex.

Structural alterations of CHR upon binding to Cu^{2+}

Circular dichroism spectroscopy was employed to monitor the structural alterations of CHR upon binding to Cu^{2+}. Figure 10a, b show the changes in CD spectra of CHR in the near UV and visible range respectively. Near UV CD spectra is characterized by quenching of the signature band at 276 nm. We also observe the emergence of new positive bands around 242 nm and 322 nm. The appearance of these new CD

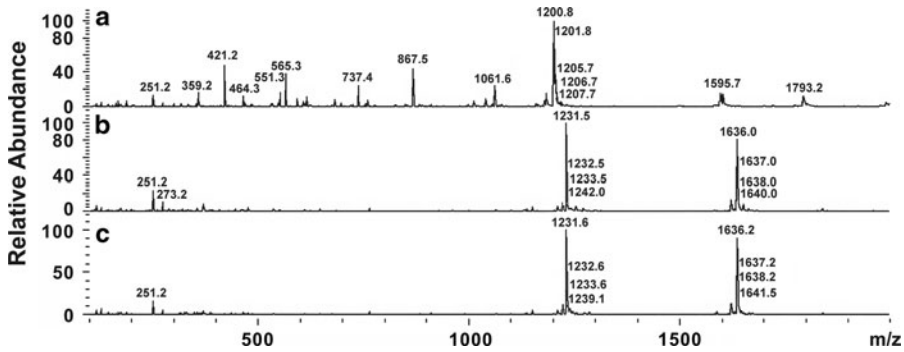

Fig. 6 **a** ESI–MS profile of unbound CHR (50 μM) in 10 mM NH_4HCO_3 buffer, pH 8.0. **b** ESI–MS profile of [$(CHR)_2$:Cu^{2+}] in 10 mM NH_4HCO_3 buffer, pH 8.0. **c** ESI–MS profile of CHR in presence of equimolar amounts of $^{63}CuCl_2$ and ^{68}ZnO in 10 mM NH_4HCO_3 buffer, pH 8.0

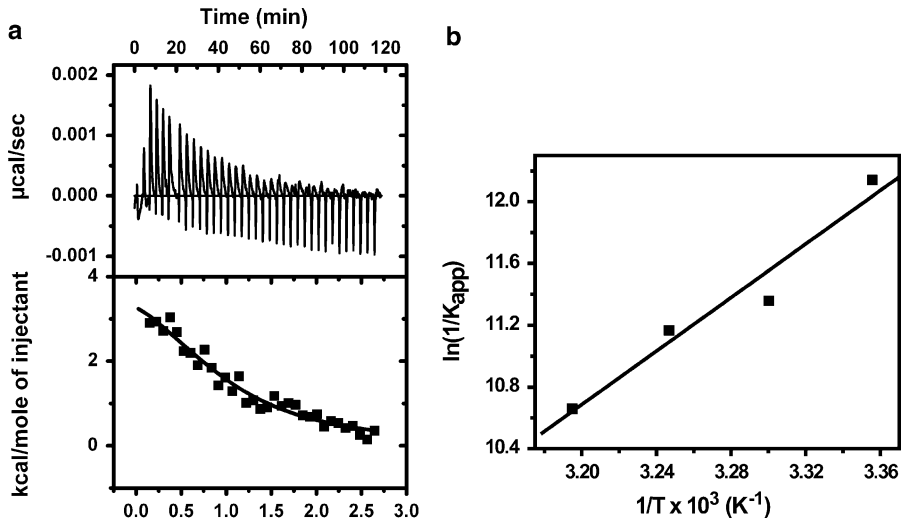

Fig. 7 **a** Thermogram for the binding of CHR to Cu^{2+} at 25°C in 10 mM Tris–HCl, pH 8.0. The top panel presents the real time data, while the lower panel shows the normalized enthalpy change for the complexation reaction. The *solid line* through the data points represents the best fit curve for the titration. **b** Plot of $\ln(1/K_{app})$ versus 1/T at 4 different temperatures (25, 30, 35 and 40°C) for the complex formation between CHR and Cu^{2+} in 10 mM Tris–HCl, pH 8.0. The *solid line* represents the best fit *linear curve* through the obtained data points

Table 3 Binding parameters for the complex formation between CHR and Cu^{2+}

System	Reaction enthalpy (kcal/mole)		Reaction entropy (cal/K/mole)		Apparent dissociation constant (K_d, μM) at 25°C	
	ITC	van't Hoff	ITC	van't Hoff	ITC	van't Hoff
CHR : Cu^{2+}	4.9 ± 0.75	−17.3 ± 1.4	39.4	−34.1	9.4	5.3
CHR : Zn^{2+}	3.4	8.0	31	37	62.5	35.2

Thermodynamic parameters for the association of CHR with Cu^{2+} and comparison of those with [$(CHR)_2$:Zn^{2+}] complex

Values for the association between CHR and Zn^{2+} is cited from (Devi et al. 2007)

bands distinguishes the structure of [$(CHR)_2$:Cu^{2+}] complex from either of [$(CHR)_2$:Mg^{2+}] and [$(CHR)_2$:Zn^{2+}] complexes (Aich et al. 1992a; Devi et al. 2007). Spectra in the visible region are characterized by quenching of intensity at 420 nm. Presence of an isoelliptic point at 362 nm corroborates the formation of a single type of CHR:Cu^{2+} complex. This is accompanied by the emergence of a broad band around 475 nm. The intensity of this band (at 50 μM Cu^{2+}) is nearly five times higher compared to that of free CHR at the same wavelength. This is a unique feature of the Cu^{2+} complex. Comparison of CD

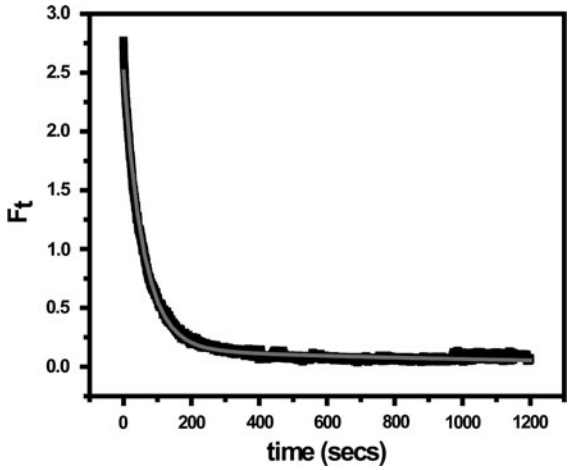

Fig. 8 Stopped-flow kinetic trace for the association of CHR (10 μM) with Cu^{2+} (600 μM) at 25°C in 10 mM Tris–HCl buffer, pH 8.0. Fluorescence intensity (F_t) is plotted against time. The *solid grey line* represents the best fit *curve* corresponding to the biphasic rate equation of $F_{540} = 0.94e^{-(0.0175\pm0.00057)t} + 0.06e^{-(0.0007\pm0.0001)t}$

spectral features with earlier reported data of [$(CHR)_2$:Mg^{2+}] and [$(CHR)_2$:Zn^{2+}] complexes show that the broad band appears at around 450 nm and its intensity at highest concentrations of Mg^{2+} and Zn^{2+} ions are lower than that of unbound CHR (Aich et al. 1992a; Devi et al. 2007).

Structure of the [$(CHR)_2$:Cu^{2+}] complex

Proton resonances were assigned to unbound CHR and to the complex from 1D and 2D (through bond connectivity—DQF-COSY and through space connectivity—NOESY) NMR data (Table 5), which were then compared with previously reported values for the unbound and bound antibiotic (Gao and Patel 1989; Sakaguchi et al. 1991; Silva et al. 1993; Silva and Kahne 1993). The data obtained were also compared with the previously reported structures of [$(CHR)_2$:Mg^{2+}] complex (Gao and Patel 1989; Silva et al. 1993; Silva and Kahne 1993). However, we did not observe any significant line broadening of proton peaks due to presence of Cu^{2+}. The resonances due to C2-H and C1′-H could not be resolved due to masking of the region by signals from HDO (around $\delta = 4.7$) (Fig. 11a). Protons from C, D rings of the trisaccharide unit seem to come in close contact with C10-H, indicating the formation of an altered conformation from that observed in case of Zn^{2+} complex (Devi et al. 2007) (Fig. 11b). We have observed changes in the chemical shift values of protons of the aliphatic side chain at C3, which are closer to the chromomycinone plane (Table 5). This suggests a gross change in the environment of the protons upon addition of Cu^{2+}. Moreover, disappearance of a number of NOE contacts present in unbound CHR suggests that the antibiotic molecules move away in order to facilitate the complex formation. The molecules change their relative position from the aggregated unbound form to facilitate the complexation reaction. On the other hand, appearance of new NOE contacts upon addition of Cu^{2+} suggests a defined arrangement of the saccharide units in the complex (Fig. 11c, d).

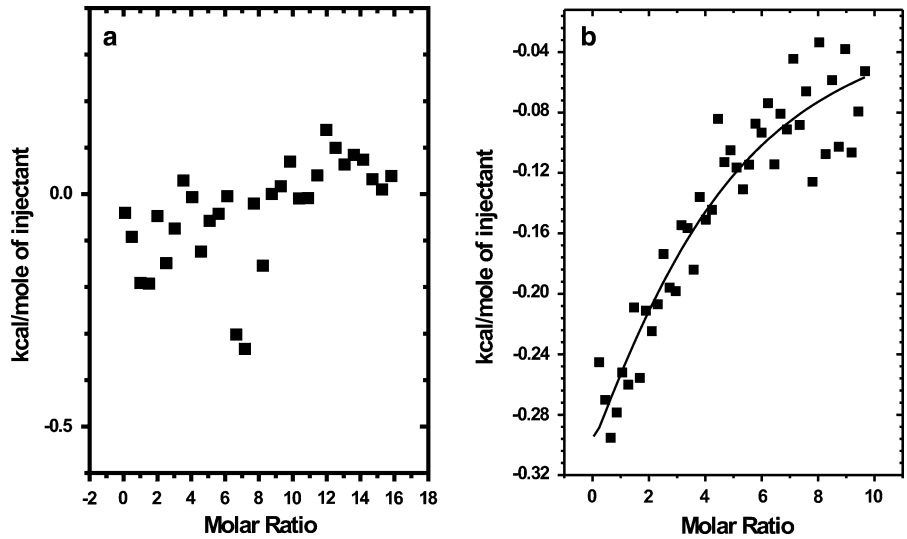

Fig. 9 **a** Normalised thermogram for the titration of 30 μM [$(CHR)_2$:Cu^{2+}] with ct DNA. **b** Normalised thermogram for the titration of 30 μM [$(CHR)_2$:Zn^{2+}] with ct DNA. The *solid line* represents the best fit curve corresponding to 'one set of sites' model for the interaction of [$(CHR)_2$:Zn^{2+}] complex with ct DNA. Both titrations were performed in 10 mM Tris–HCl, pH 8.0 at 25°C

Table 4 Interaction of $[(CHR)_2:Zn^{2+}]$ complex with double helical DNA

System	Stoichiometry, N (no. of bases/molecule of the complex)	ΔH (kcal/mole)	ΔS (cal/K/mole)	K_{app} (μM)
$[(CHR)_2:Zn^{2+}]$-ct DNA	3.41 ± 0.09 (5.5 ± 0.5)	−2.25 ± 0.28	12.7	37.03 (19)

Thermodynamic parameters for association of $[(CHR)_2:Zn^{2+}]$ complex with ct DNA

Numbers in the parentheses are the values for the association of $[(MTR)_2:Zn^{2+}]$ complex with ct DNA as reported earlier from our laboratory by means of fluorescence spectroscopic measurements (Das and Dasgupta 2005)

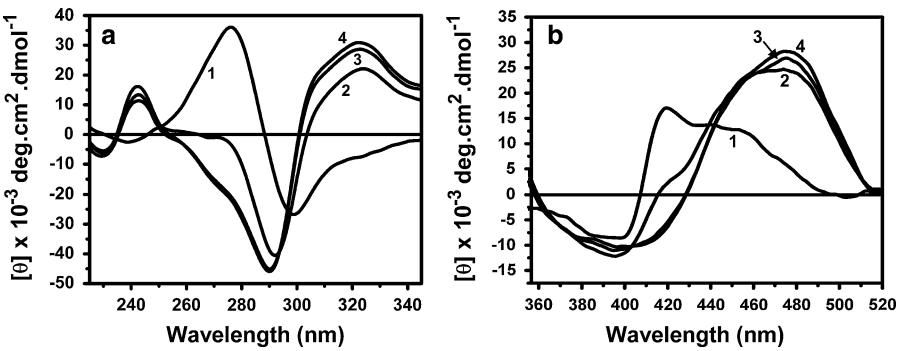

Fig. 10 CD spectra of 10 μM CHR (*curve 1*) and on addition of 5 μM (*curve 2*), 15 μM (*curve 3*) and 50 μM (*curve 4*) Cu^{2+} **a** in the near UV range and **b** in the visible range. All spectra were recorded at 25°C in 10 mM Tris–HCl, pH 8.0. The spectra reported are an average of four scans

Following observations lead to the determination of the structure of $[(CHR)_2:Cu^{2+}]$ complex and relative orientation of different parts of CHR molecule in the same. Comparison with the NMR data reported earlier for the complexes with Mg^{2+} and Zn^{2+} (Devi et al. 2007; Gao and Patel 1989; Silva et al. 1993; Silva and Kahne 1993), suggests that the Cu^{2+} complex possibly adopts geometry different from the conventional octahedral or tetrahedral structure.

(i) Chemical shift values for the C7-CH_3 protons do not change significantly upon addition of Cu^{2+} indicating that this region is located far from the coordination site. Absence of NOE contacts also implies that this region of the molecule is not involved in complex formation.

(ii) Development of a new NOE contact between a proton from the trisaccharide moiety and C10-H (Fig. 11b) indicates geometry, where the sugar protons of one molecule come in close contact with the C10-H of another molecule. It also indicates that the O1 and O9 atoms responsible for coordination are in *trans* orientation with respect to the metal ion.

(iii) Furthermore, appearance of new NOE connectivities between some of the A and B ring sugar protons and C4-H (Fig. 11c) confirms the *trans* orientation of the CHR molecules in the complex.

(iv) Appearance of NOE contacts between different protons (H1, H2, H5, H6) of the B ring of the disaccharide unit and protons from the aliphatic side chain (C3′-H, C4′-H, C4′-CH_3) (Fig. 11d) not only confirms our earlier observations but also indicates that the sugar moieties of one molecule of CHR is crowded over the acyclic part of another molecule in the complex. We also observe a significant downfield shift of C4′-H (Δ 0.13 ppm), which indicates that this region lies just outside the shielding effect of the coordination sites.

(v) An interesting observation is that new NOE contacts develop between some protons of the D sugar rings (DC1/C2″-H(s)) and C3/C4′-H(s), which might arise from the formation of a structure where more than one unit of the complex come close, as is observed in ESI–MS experiments, since involvement of the above parts from the same CHR molecule or from two molecules of one $[(CHR)_2:Cu^{2+}]$ unit would accompany severe conformational and steric strain. Considering the above observations, the trisaccharide unit has no chance to develop NOE contacts with C3/C4′-H(s) and therefore this explanation seems to be most plausible.

Table 5 NMR study of CHR and [$(CHR)_2$:Cu^{2+}]

Atom	δ values, ppm (CHR)	δ values, ppm [$(CHR)_2$:Cu^{2+}]
C2H	–	–
C3H	2.43	2.39
C4H(a)	3.13	3.20
C4H(e)	2.69	2.73
C5H	6.10	6.10
C10H	6.43	6.44
$C7CH_3$	1.82	1.79
C1′H	–	–
$C1'OCH_3$	3.23	3.22
C3′H	3.10	3.08
C4′H	3.29	3.42
$C4'CH_3$	1.20	1.25
B-ring OCH_3	3.27	3.28
A-ring OAc	2.06	2.057
E-ring OAc	2.11	2.112

Chemical shift values for CHR and [$(CHR)_2$:Cu^{2+}]

Discussion

There are three important considerations which led us to the current study. First, Cu^{2+} accumulation resulting from its misbalanced homeostasis in the cell has been implied in various pathological conditions such as Wilson's disease, Menke's disease, Alzheimer's disease, some cases of tumor progression, etc. (Valko et al. 2006; Waggoner et al. 1999). Hypercupremia has also been implicated in schizophrenia, adult insomnia and a host of cardiovascular disorders (Pfeiffer and Mailloux 1987). Second, copper chelating drugs are gaining importance as a possible treatment for such diseases (Daniel et al. 2004; Di Vaira et al. 2004). Third, there has been a recent spate of studies to probe alternative therapeutic potential of the structurally related generic drug, Mithramycin (Chakraborty et al. 2008). Studies show that these aureolic acid antibiotics can cross the blood–brain barrier, which makes them more important (Ferrante et al. 2004). The present report shows that CHR binds to Cu^{2+} like other bivalent metal ions, Mg^{2+} and Zn^{2+}, in vitro. However the structures, specifically the coordination geometry, of the antibiotic moiety around the bivalent metal ions are different. As a result we have come across the novel observation that selectively [$(CHR)_2$:Cu^{2+}] complex does not bind to double helical DNA. Earlier studies from our laboratory and other laboratories have established that [$(drug)_2$:metal ion] complex is the biological species that binds to and inhibits the template property of DNA (Chakrabarti et al. 2000; Das and Dasgupta 2005; Hou et al. 2004). Our present results imply that under in vivo conditions, there is a partitioning of the molecule between DNA binding and association with Cu^{2+} only. The rate of association of CHR with the three metal ions reported earlier (Aich et al. 1992a; Devi et al. 2007) and in this paper suggest the absence of preferential association with the metal ions from kinetics standpoint. However, the K_d values as shown in Table 2 suggest that CHR has strongest affinity for Cu^{2+}. This reinforces our earlier proposition. It is further corroborated from the fact that CHR preferentially binds to Cu^{2+} and forms [$(CHR)_2$:Cu^{2+}] complex in presence of equimolar amount of Zn^{2+}, as is observed from ESI–MS measurements. This conclusion assumes further significance in view of the possibility of employing the aureolic acid group of antibiotics as potential chelator (either alone or in combination therapy) in diseases originating from Cu^{2+} accumulation. The above points are discussed in details below.

Optical spectroscopic studies, absorbance, fluorescence and CD, provide direct evidence for the binding. Binding of CHR to Cu^{2+} is associated with a broadening and red shift of the absorbance spectra. Two possible factors might lead to the above features. First, red shift of the absorbance spectra can occur due to the stabilization of the π^* orbital, thereby reducing the energy gap for the $\pi \rightarrow \pi^*$ transition. The stabilization of the π^* orbital could be a sequel to the ligand to metal charge transfer (LMCT) (Huheey et al. 1978). Observed broadening could also result from the close proximity of the chromophores, when more than two molecules of the antibiotic are present per molecule of the complex. Reduced quantum yield noted in the fluorescence emission spectra of CHR in presence of the metal ion could also be an outcome of the proximity of the chromophores upon complex formation. Such proximity of fluorophores within the complex can cause deactivation of a singlet excited state leading to observed quenching and reduced quantum yield of CHR upon addition of Cu^{2+} (Aich et al. 1992b). Similar changes were reported for the association of CHR with Mg^{2+} and Zn^{2+} (Aich et al. 1992a; Devi et al. 2007). Stoichiometry of 2:1 (in terms of CHR:Cu^{2+}) estimated by continuous

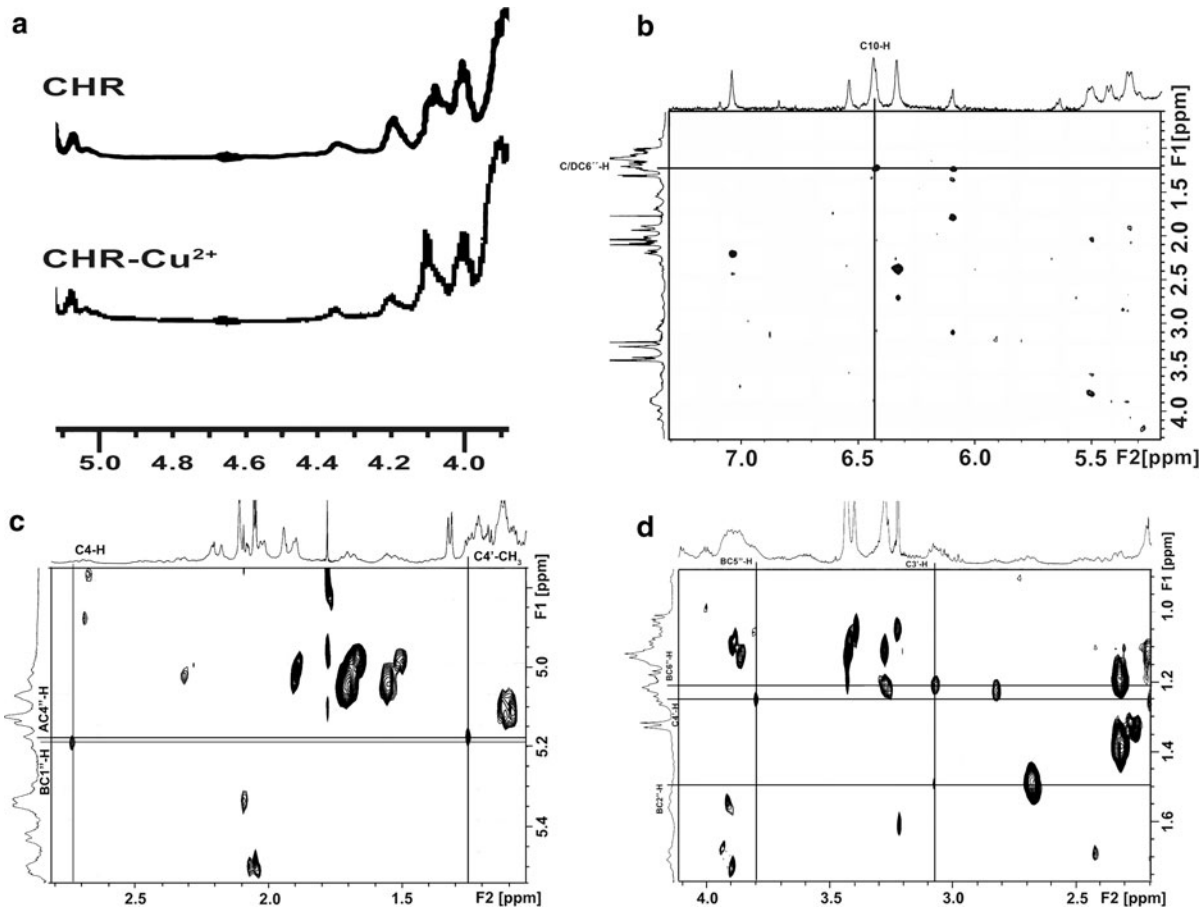

Fig. 11 **a** Masking of resonance signals around $\delta = 4.7$ ppm by DOH. **b** NOE contact between C10-H and a sugar proton. **c** NOE contacts between C4-H and C4′-CH_3 and protons from the disaccharide unit. **d** NOE contacts between C3′-H and sugar protons. All NMR spectra were recorded at 25°C in 20 mM K-phosphate buffer, pH 8.0

variation method is consistent with the proposition of the proximity of two CHR moieties in the complex and hence the trend in the optical spectroscopic studies. Formation of the [$(CHR)_2$:Cu^{2+}] complex in solution was conclusively demonstrated by ESI–MS using monoisotopic $^{63}CuCl_2$. It was shown in ESI–MS measurements that CHR forms a stable [$(CHR)_2$:Cu^{2+}] complex in solution. Formation of the CHR dimer as monitored by ESI–MS could be explained by Scheme 1.

Evaluation of the binding parameters shows that CHR binds to Cu^{2+} with a micromolar order of affinity. The discrepancy of the values for the thermodynamic parameters obtained by ITC and van't Hoff plot is noteworthy. Similar discrepancy was reported for the formation of complex between CHR and Zn^{2+} (Devi et al. 2007). The significant discrepancy in the enthalpy changes as obtained by two different methods indicate that the association involves linked equlibria shown below:

$$\mathrm{CHR} + \mathrm{Cu}^{2+} \leftrightarrows [\mathrm{CHR{:}Cu}^{2+}] \overset{\mathrm{CHR}}{\leftrightarrows} [(\mathrm{CHR})_2 : \mathrm{Cu}^{2+}]$$

The above proposal suggests progressive formation of 1:1 and 2:1 complexes between the antibiotic and Cu^{2+}. The observed biphasic kinetics supports the proposition. However, the present kinetic data are not sufficient for characterization of the two steps in terms of the molecular processes or an additional spectroscopically silent step as reported for Zn^{2+} (Devi et al. 2007). One of the two steps might be spectroscopically silent. That is why we do not get the overall enthalpy

change by means of van't Hoff plot. Calorimetric titration shows that the binding is endothermic in nature and entropy driven at room temperature. The high value of the reaction entropy could be ascribed to the displacement of bound water associated with the antibiotic into the bulk solvent due to complex formation. Structural alteration of the antibiotic upon complex formation gives rise to the change in the CD spectra in near UV and the visible region. Changes in the CD spectra suggest that the environment of the chromophore is grossly affected due to the complex formation. This trend is evident in NMR experiments also, as discussed below. Moreover, comparison of the CD spectral features of [$(CHR)_2$:Cu^{2+}] with those of the earlier reported Mg^{2+} and Zn^{2+} complex suggests that the structure formed as a result of complex formation with Cu^{2+} is significantly different from the conformation adopted by either of [$(CHR)_2$:Mg^{2+}] and [$(CHR)_2$:Zn^{2+}].

We have considered the octahedral geometry as our starting point, since Cu^{2+} is present in an octahedral geometry in $CuSO_4.5H_2O$. We examined whether the two energetically favorable octahedral conformations (I and II, as shown below) that the complex can adopt (Silva and Kahne 1993), could be explained by our NMR data. Although there is a chance that the trisaccharide moiety of one antibiotic molecule might come in close contact with the aromatic rings of the other one (in structure I), but it is very unlikely that only a single proton (C/DC6″-H) from the trisaccharide unit comes closer to C10-H. Moreover, development of NOE contacts between C4-H and AC4″-H and BC1″-H as well as those between aliphatic side chain protons and those from the disaccharide unit (as described in the results section) cannot be explained by either of the structures, I or II.

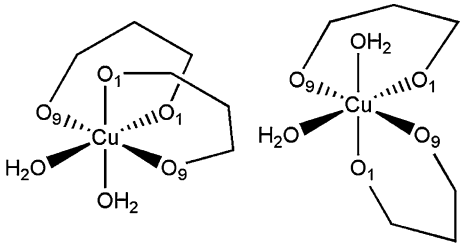

I II

The crowding of the disaccharide moiety around the aliphatic side chain at C3 as a result of the *trans*

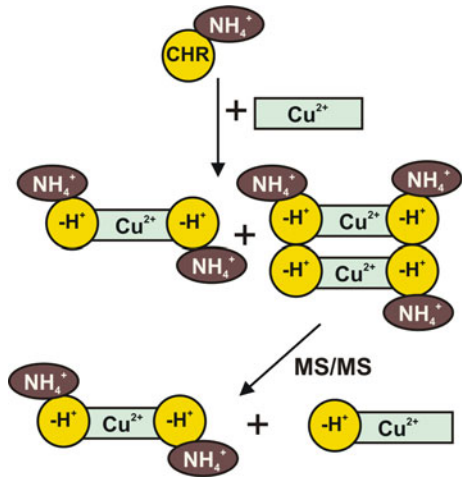

Scheme 1 Formation of a stable [$(CHR)_2$:Cu^{2+}] complex as observed by ESI–MS measurements

orientation is difficult to conceive in either of the above two structures. In view of our observations, we suggest that the [$(CHR)_2$:Cu^{2+}] complex adopts a distorted octahedral geometry. Formation of a tetrahedral geometry is also improbable. The relative orientation of the CHR molecules obtained here is unlike the proposed tetrahedral model for [(antibiotic)$_2$:Zn^{2+}] complex (from a comparison of NOE data in case of Cu^{2+} and Zn^{2+}, as reported earlier) (Devi et al. 2007). Downfield shift of C4′-H observed here also does not support the tetrahedral model. Further evidence of [$(CHR)_2$:Cu^{2+}] complex adopting a structure other than the tetrahedral arrangement is obtained from CD spectroscopic results. The notable bivalent metal ion dependent difference in the alteration of CD spectra of CHR in both visible and near UV regions may be ascribed to different structures of the [$(CHR)_2$:M^{2+}] complexes.

Further support for our proposition comes from earlier studies that Cu^{2+} in general forms complexes with a coordination number of 6, but regular octahedral structures are not the rule (Daniel et al. 2004). Again Cu^{2+} has a $[Ar]3d^9$ electronic configuration, which renders its complexes with non-zero crystal field stabilization energy. This provides the Cu^{2+} complexes with a finite energy barrier between different possible conformations and hence, the structure once assumed remains intact without any external perturbation.

A previous report exploring the effect of spermine on the DNA binding efficacy of different [CHR:metal] complexes has shown that [$(CHR)_2$:Cu^{2+}] complex binds to DNA with a very low efficacy (Lu et al. 2009). However, the studies were performed using biotinylated synthetic hairpin DNA with the following sequence—biotin-d(TTGGCCAATGTTTGGCCAA). Current report involves linear B-type double helical DNA without any hairpin structure. It shows that the [$(CHR)_2$:Cu^{2+}] complex does not interact with linear double stranded DNA, unlike other two metal complexes reported earlier from our laboratory (Aich et al. 1992b; Devi et al. 2007). As indicated from calorimetric titrations, [$(CHR)_2$:Cu^{2+}] complex does not interact with ct DNA ($\sim$50% GC content), nor does it interact with 5′-CCGGCGCCGG-3′, which contains the possible binding motifs required for binding of CHR-metal complexes to DNA (Van Dyke and Dervan 1983). Previous studies on structure of the metal complexes formed by CHR as well as those of the [$(CHR)_2$:M^{2+}]-DNA complexes show that the arrangement of the ligands around the metal centre is of prime importance (Hou et al. 2004; Silva and Kahne 1993). The coordination around the metal ion in case of [$(CHR)_2$:Mg^{2+}] complex has octahedral geometry. The metal ion binds to the two oxygen atoms of each chromophore and two water molecules act as the fifth and sixth ligands. In addition, other bridging water molecules that mediate the interaction between the CHR and DNA in the duplex were also observed in the crystal structure (Hou et al. 2004). The right handed twist conformation adopted by the complex, complement the DNA double helical turn in binding to the minor groove (Gao and Patel 1989; Hou et al. 2004; Sakaguchi et al. 1991; Silva et al. 1993; Silva and Kahne 1993). Lu et al. has proposed a square planar structure for the [$(CHR)_2$:Cu^{2+}] complex from MD simulation studies (Lu et al. 2009). However, the sugar moieties of the antibiotics were not taken into account for the computation of the structure. These sugar moieties play a very important role in determining the structure of the dimer and its DNA binding property (Devi et al. 2007; Silva et al. 1993; Silva and Kahne 1993). Square planar geometry of the [$(CHR)_2$:Cu^{2+}] complex is also not conducive to binding of the complex to double helical DNA. Our proposal of distorted octahedral structure of the complex is not complementary to the DNA surface.

Acknowledgments We thank Prof. Siddhartha Roy, Director, Indian Institute of Chemical Biology (IICB), Kolkata for allowing us to access the central NMR facility and Mr. E. Padmanabhan for his technical assistance. We thank Prof. Toshiharu Hase, Director, Institute for Protein Research (IPR), Osaka University for inviting SL through the International Collaborative Research Programme with Professor Takao to perform the ESI–MS experiments. We also thank Ms. Parijat Majumder for critical reading of the manuscript. This work was supported by the intramural grant (Molecular Mechanism of Disease and Drug Action (MMDDA) project) [Grant number: 11-R&D-SIN-5.04] from Department of Atomic Energy, Govt. of India.

References

Aich P, Sen R, Dasgupta D (1992a) Interaction between antitumor antibiotic chromomycin A3 and Mg2 + I Evidence for the formation of two types of chromomycin A3-Mg2 + complexes. Chem Biol Interact 83(1):23–33

Aich P, Sen R, Dasgupta D (1992b) Role of magnesium ion in the interaction between chromomycin A3 and DNA: binding of chromomycin A3-magnesium (2 +) complexes with DNA. Biochemistry 31(11):2988–2997

Baguley B (1982) Nonintercalative DNA-binding antitumour compounds. Mol Cell Biochem 43(3):167–181

Behr W, Honikel K, Hartmann G (1969) Interaction of the RNA polymerase inhibitor chromomycin with DNA. Eur J Biochem 9(1):82–92

Chakrabarti S, Aich P, Sarker D, Bhattacharyya D, Dasgupta D (2000) Role of Mg2 + in the interaction of anticancer antibiotic, chromomycin A3 with DNA: does neutral antibiotic bind DNA in absence of the metal ion? J Biomol Struct Dyn 18(2):209

Chakraborty H, Devi PG, Sarkar M, Dasgupta D (2008) Multiple functions of generic drugs: future perspectives of aureolic acid group of anti-cancer antibiotics and non-steroidal anti-inflammatory drugs. Mini Rev Med Chem 8(4):331–349

Cons BM, Fox KR (1989) High resolution hydroxyl radical footprinting of the binding of mithramycin and related antibiotics to DNA. Nucleic Acids Res 17(14):5447–5459

Daniel KG, Harbach RH, Guida WC, Dou QP (2004) Copper storage diseases: Menkes, Wilsons, and cancer. Front Biosci 9:2652–2662

Das S, Dasgupta D (2005) Binding of (MTR) 2Zn2 + complex to chromatin: a comparison with (MTR) 2Mg2 + complex. J Inorg Biochem 99(3):707–715

Devi PG, Pal S, Banerjee R, Dasgupta D (2007) Association of antitumor antibiotics, mithramycin and chromomycin, with Zn (II). J Inorg Biochem 101(1):127–137

Di Vaira M, Bazzicalupi C, Orioli P, Messori L, Bruni B, Zatta P (2004) Clioquinol, a drug for Alzheimer's disease specifically interfering with brain metal metabolism: structural characterization of its zinc (II) and copper (II) complexes. Inorg Chem 43(13):3795–3797

Fernandez-de-Cossio J, Gonzalez LJ, Satomi Y, Betancourt L, Ramos Y, Huerta V, Besada V, Padron G, Minamino N,

Takao T (2004) Automated interpretation of mass spectra of complex mixtures by matching of isotope peak distributions. Rapid Commun Mass Spectrom 18(20):2465–2472. doi:10.1002/rcm.1647

Ferrante RJ, Ryu H, Kubilus JK, D'Mello S, Sugars KL, Lee J, Lu P, Smith K, Browne S, Beal MF (2004) Chemotherapy for the brain: the antitumor antibiotic mithramycin prolongs survival in a mouse model of Huntington's disease. J Neurosci 24(46):10335

Gao XL, Patel DJ (1989) Solution structure of the chromomycin-DNA complex. Biochemistry 28(2):751–762

Gochin M (1998) Nuclear magnetic resonance characterization of a paramagnetic DNA-drug complex with high spin cobalt; assignment of the 1H and 31P NMR spectra, and determination of electronic, spectroscopic and molecular properties. J Biomol NMR 12(2):243–257

Hou MH, Robinson H, Gao YG, Wang AHJ (2004) Crystal structure of the [Mg2 + (chromomycin A3) 2]–d (TTGGCCAA) 2 complex reveals GGCC binding specificity of the drug dimer chelated by a metal ion. Nucleic Acids Res 32(7):2214

Huheey JE, Keiter EA, Keiter RL, Medhi OK (1978) Inorganic chemistry: principles of structure and reactivity. Harper & Row, New York

Lombo F, Menendez N, Salas JA, Mendez C (2006) The aureolic acid family of antitumor compounds: structure, mode of action, biosynthesis, and novel derivatives. Appl Microbiol Biotechnol 73(1):1–14. doi:10.1007/s00253-006-0511-6

Lu WJ, Wang HM, Yuann JM, Huang CY, Hou MH (2009) The impact of spermine competition on the efficacy of DNA-binding Fe(II), Co(II), and Cu(II) complexes of dimeric chromomycin A(3). J Inorg Biochem 103(12):1626–1633. doi:10.1016/j.jinorgbio.2009.09.003

Olivares M, Uauy R (1996) Copper as an essential nutrient. Am J Clin Nutr 63(5):791S

Pfeiffer CC, Mailloux R (1987) Excess copper as a factor in human diseases. J Orthomol Med 2(3):171–182

Reyzer ML, Brodbelt JS, Kerwin SM, Kumar D (2001) Evaluation of complexation of metal-mediated DNA-binding drugs to oligonucleotides via electrospray ionization mass spectrometry. Nucleic Acids Res 29(21):e103

Sakaguchi R, Katahira M, Kyogoku Y, Fujii S (1991) An NMR study on the conformation of a deoxyoligonucleotide duplex, d(GGGGCCCC)2, and its complex with chromomycin. J Biochem 109(2):317–327

Silva DJ, Kahne DE (1993) Studies of the 2: 1 chromomycin A3-Mg2 + complex in methanol: role of the carbohydrates in complex formation. J Am Chem Soc 115(18):7962–7970

Silva DJ, Goodnow R Jr, Kahne D (1993) The sugars in chromomycin A3 stabilize the Mg(2 +)-dimer complex. Biochemistry 32(2):463–471

Sleiman SF, Langley BC, Basso M, Berlin J, Xia L, Payappilly JB, Kharel MK, Guo H, Marsh JL, Thompson LM, Mahishi L, Ahuja P, MacLellan WR, Geschwind DH, Coppola G, Rohr J, Ratan RR (2011) Mithramycin is a gene-selective Sp1 inhibitor that identifies a biological intersection between cancer and neurodegeneration. J Neurosci 31(18):6858

Valko M, Rhodes C, Moncol J, Izakovic M, Mazur M (2006) Free radicals, metals and antioxidants in oxidative stress-induced cancer. Chem Biol Interact 160(1):1–40

Van Dyke M, Dervan P (1983) Chromomycin, mithramycin, and olivomycin binding sites on heterogeneous deoxyribonucleic acid. Footprinting with (methidiumpropyl-EDTA) iron (II). Biochemistry 22(10):2373

Waggoner DJ, Bartnikas TB, Gitlin JD (1999) The role of copper in neurodegenerative disease. Neurobiol Dis 6(4): 221–230